ARTICLE NO. 78-517

Vibration Techniques for Definition of Practical Boundary Conditions in Stiffened Shells

Josef Singer* and Haim Abramovich†
Technion-Israel Institute of Technology, Haifa, Israel

A vibration correlation technique, consisting essentially of experimental determination of the frequencies under load and assessment of equivalent elastic restraints, developed earlier for stringer-stiffened shells on laboratory-type end rings, has been extended to realistic boundary conditions. Six shells with end conditions, simulating typical missile joints, have been tested and analyzed. "Lumping" of end effects has been studied and results have been compared with tests of similar shells on laboratory-type end rings with prescribed load eccentricity. A method for detection of load eccentricity from vibration tests and assessment of equivalent end restraints has been developed.

Nomenclature

A_l = cross-sectional area of stringer
b_l = stringer spacing
$C4$ = clamped boundary conditions ($u=v=w=w_{,x}=0$)
c_l = width of stringer
d_l = height of stringer
E = Young's modulus
e_l = stringer eccentricity (distance from shell middle surface to centroid of stringer)
$\bar{e}$ = average eccentricity of loading (distance from shell middle surface to the point of load application)
f = frequency
f_{SS4_L} = frequency predicted by linear theory for *SS4* boundary conditions
$f_{SS4+\bar{e}}$ = frequency predicted by BOSOR 3 or 4 in the presence of load eccentricity
h = thickness of shell
I_{ll} = moment of inertia of stringer cross section about its centroidal axis
k_l = nondimensional elastic axial restraint
k_A = $(f_{SS4+\bar{e}}/f_{SS4_L})^2$, theoretical frequency ratio squared
k_B = $(f/f_{SS4_L})^2$, experimental frequency ratio squared
k_C = k_B/k_A, equivalent boundary condition factor
L = length of shell
m = number of half longitudinal waves
n = circumferential wave number
P = axial compressive load
P_{cr} = theoretical buckling load
P_{exp} = experimental buckling load
P_{post} = experimental postbuckling load
P_{sp} = calculated buckling load for a shell with elastic axial restraint
R = radius to shell middle surface
$SS3$ = classical simple support ($w=M_x=N_x=v=0$)
$SS4$ = axially restrained simple support ($w=M_x=u=v=0$)
Z = $(1-\nu^2)^{1/2}(L/R)^2(R/h)$, Batdorf shell parameter
ν = Poisson's ratio
ρ = "linearity," ratio between experimental buckling load and the theoretical value predicted by linear theory
$\sigma_{0.001}$ = 0.1% offset yield stress

Presented as Paper 78-517 at the AIAA/ASME 19th Structures, Structural Dynamics and Materials Conference, Bethesda, Md., April 3-5, 1978; submitted Aug. 14, 1978; revision received Jan. 25, 1979.

Index categories: Structural Stability; Structural Dynamics.

*Professor, L. Shirley Tark Chair of Aircraft Structures, Dept. of Aeronautical Engineering. Fellow AIAA.

†Graduate Student, Dept. of Aeronautical Engineering.

I. Introduction

THE influence of boundary conditions on the buckling of stiffened shells is as important as that of the initial imperfections and may even be predominant.[1,2] A better definition of the boundary conditions will therefore lead to more accurate predictions of buckling loads. Since the boundary conditions have a similar effect on the lower natural frequencies of vibrations of stiffened shells,[3-5] correlation between vibration and buckling of stiffened cylindrical shells was studied extensively at the Technion.[2,5-10] These studies yielded an experimental technique for the definition of the boundary conditions.[2,6,7]

The vibration correlation technique consists essentially of an experimental determination of the lower natural frequencies for a loaded shell and assessment of equivalent elastic restraints, which represent the real boundary conditions. These are then employed for calculation of the buckling loads. The method was developed for axially loaded stringer-stiffened shells mounted on typical laboratory-type end rings. It was perfected in a broad test program and yielded a very significant reduction in the experimental scatter (see, for example, Fig. 17 of Ref. 6). The method recently has also been extended to eccentrically applied axial load[9] and to external pressure loading.[10]

The method is, however, of limited value unless it can also be applied to realistic boundary conditions. Considerable effort has therefore been directed to its extension to shells with end supports simulating joints employed in actual aircraft and missile construction. The present paper summarizes a study on stringer-stiffened cylindrical shells riveted to end rings that represent a typical missile clamp joint.

The change to practical boundary conditions required improvements in the test rig and test technique for efficient excitation and scanning of the vibration modes, which are discussed in the next section. A more basic problem encountered is, however, the "lumping" of different boundary effects. In the earlier work with laboratory-type end conditions it was realized that the equivalent elastic restraints also include the imperfections of the shell and the "lumping" was studied[2,7,4]; however, these two phenomena have similar effects on buckling and vibrations. Here, a third phenomenon—eccentricity of loading—is introduced, for which correlation between vibration and buckling is more

complicated.[9] The eccentricity of loading is not immediately apparent in the design of the joint, but is introduced indirectly through the rings and its magnitude is not known. Here it was initially inferred from the buckling behavior of the shells tested, which was nonviolent, without noise, and with a small drop in load at buckling. Such behavior typifies significant load eccentricity as observed in earlier experimental studies.[12] It was later verified on two shells with special closely spaced strain gages which detected corresponding bending strains near the edges.

Observation of load eccentricity at buckling, however, is not sufficient. For nondestructive determination of the actual boundary condition, one has to be able to detect the load eccentricity from vibrations at low loads. This has been one of the aims of the present study. The resultant nondestructive technique for the detection of load eccentricity is then developed into a method for definition of practical boundary conditions. Once defined, the effective boundary conditions are employed as before[6,7] for improved prediction of the buckling loads.

For the theoretical predictions "smeared-stiffener" theory,[14,15] which assumes the stiffeners to be "smeared" or distributed over the surface of the shell, is used. For the usual vibration correlation technique a linear Flügge-type theory[7,13] is employed, although the Donnell theory would yield practically identical results.[13] In the presence of load eccentricity, a theory that considers nonlinear prebuckling deformation and load eccentricity has to be used. Here, a multipurpose program BOSOR 3[16] or BOSOR 4,[17] based on the finite-difference energy method, is employed.

II. Test Specimens and Boundary Conditions

The primary aim of the present study was the extension of the vibration correlation method to shells on practical aerospace-type supports. The test program centered, therefore, on a series of six integrally stringer-stiffened cylindrical shells riveted to end rings that simulate a typical missile clamp joint. The shells (see Fig. 1) are similar to those tested earlier on laboratory-type end rings in order to facilitate comparison between the two types of boundary conditions. The dimensions of these AB shells are presented in Table 1. They are made from 7075-T6 aluminum alloy tubes (10 in. diameter and ½ in. wall thickness) and by a manufacturing technique developed earlier[18] for accurate specimens. Their material properties are[18] $E = 7500$ kg/mm^2, $\nu = 0.3$, and $\sigma_{0.001} = 54$ kg/mm^2.

The boundary conditions, shown in Fig. 2, represent a missile clamp joint, but with the clamp turned to the inside for experimental convenience. Instead of the external circumferentially tightened clamp that would appear in practice, clamping of the end rings (G in Fig. 2) riveted to the shell and the support rings (C) is achieved here by two relatively heavy rings (F), which are tightened vertically by a series of bolts (D). Distance pieces (E) are placed on the inside of the clamping rings to prevent their tilting radially. The joint is designed to transmit the load from the center of the support to the midsurface of the shell without any nominal load eccentricity. In reality, however, an unknown amount of load eccentricity is introduced, which depends on the stiffness of the parts of the joint and on the exact manner of tightening of the clamping rings. The support rings are clamped to the top and bottom base plates (A) by grooves filled with Cerrobend (B).

In the study of the load eccentricity, the results are compared with tests of similar shells with prescribed load eccentricity,[9] achieved by applying the load through the

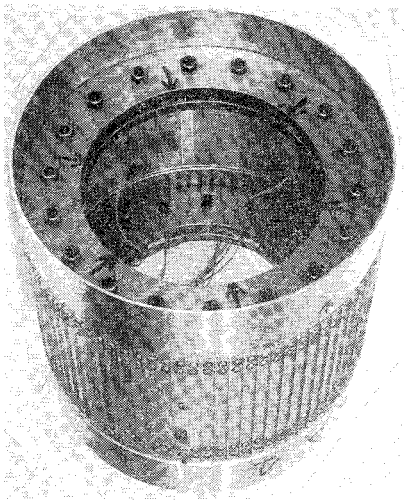

Fig. 1 Stringer-stiffened shell with ends simulating a practical aerospace joint.

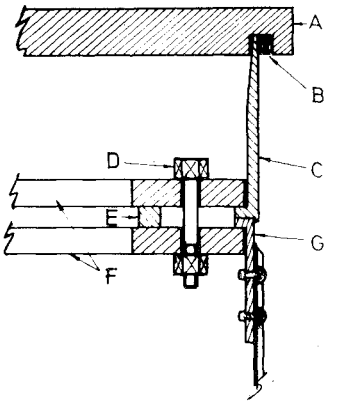

Fig. 2 Details of "practical" boundary conditions of AB shells.

Table 1 Dimensions and properties of AB shells

Shell[a]	h,mm	L, mm	R/h	L/R	Z	d_1, mm	b_1/h	A_1/b_1h	I_{11}/b_1h^3	$-e_1/h$
AB1	0.257	110	467	0.92	377	1.779	34.63	0.70	2.80	3.96
AB2	0.253	110	475	0.92	384	1.758	35.18	0.70	2.83	3.97
AB3	0.253	154	475	1.28	742	1.748	35.18	0.70	2.78	3.95
AB4	0.253	154	475	1.28	742	1.742	35.18	0.70	2.75	3.94
AB5	0.252	130	477	1.08	531	1.700	35.32	0.68	2.59	3.87
AB6	0.254	130	473	1.08	526	1.485	35.04	0.59	1.68	3.42

$R = 120.1$ (mm), $b_1 = 8.9$ (mm), $c_1 = 0.9$ (mm) except shell AB5, where $c_1 = 0.8$ (mm)
$E = 7500$ (kg/mm^2), $\nu = 0.3$
Material: Aluminum alloy 7075-T6

[a] All shells are stiffened by integral external stringers.

stringers. The details of load application for these shells are shown in Figs. 1 and 2 of Ref. 9 or Fig. 9 of Ref. 2. The specimens were manufactured in triplets, consisting of three shells made from one blank, with three kinds of edges. In the one kind of edge the load is applied through the midskin; whereas for the other kinds of edges the load is applied through the tip of the stringers or through an intermediate point along the depth of the stringer. These cases represent therefore, prescribed external load eccentricities.[2,9,12] Special end rings, accurately fitted to the shell edges, restrain the radial displacement of the shell edge or stringers. The dimensions of the comparison shells, RO-25–RO-30 given in Table 1 of Ref. 9, are: $(R/h) = 464\text{-}479$, $(L/R) = 1.08$, $Z = 518\text{-}535$, and $(A_1/b_1 h) = 0.38\text{-}0.60$, and are very similar to those of the AB shells.

III. Experimental Technique and Results

The test rig and the experimental procedure is essentially that employed earlier in the development of the vibration correlation technique,[2,5-9] but with some improvements. Figure 3 shows the modified test setup and a brief description follows. Vibrations of the shell are excited by a driver regulated by an outside oscillator and the noise emitted by the vibrating shell is picked up by a microphone positioned outside the shell. The excitation frequency is changed and resonance is detected by Lissajous figures, or output amplification, on the oscilloscope. With reasonance identified, the mode of vibration is mapped by scanning the shell with the microphone and plotting its reading versus its circumferential and axial position on X-Y recorders. The load is applied with a screw jack and measured by a load cell, and the load distribution is checked with an array of five pairs of uniformly spaced strain gages. In order to verify the presence of load eccentricity, additional strips of five closely spaced strain gages were bonded near the edges in some shells, as discussed in detail later.

The first two shells tested, AB1 and AB3, were excited, as in earlier tests, by an acoustic driver installed inside the shell. In the first shell, AB1, difficulties were encountered in identification and separation of the resonant modes. These were partly eliminated in the AB3 test by addition of a narrow band filter. After these two shells were tested, however, a more radical remedy was sought.

Instead of the acoustic driver, direct contact excitation with an electromagnetic driver suspended on springs outside the shell was tried. Two series of nondestructive intermediate tests were carried out on shell AB5 (before being riveted to end rings) mounted on laboratory-type end rings, one on "simple supports" and one "clamped" (in grooves filled with Cerrobend), to compare the vibration modes obtained by acoustic excitation and electromagnetic contact excitation. In these tests, detection of resonance by an accelerometer instead of the microphone was also compared. The details of all these comparison tests are presented in the extended version of the paper.[21] The main conclusion that emerged was that direct-contact excitation is superior for "clean" vibration of the shell alone to acoustic excitation, which induces vibrations of the whole system of shell and end rings. It was also found that the small mass of the contact leg of the electromagnetic shaker has only a negligible effect on the frequencies and mode shapes. Furthermore, the use of an accelerometer for detection of resonance instead of the microphone is not justified, since it yields only a very slight improvement. The direct-contact electromagnetic driver was, therefore, employed in all the remaining tests of the AB shells on practical boundary conditions, and was also used in a concurrent test program of external pressure loading.[10]

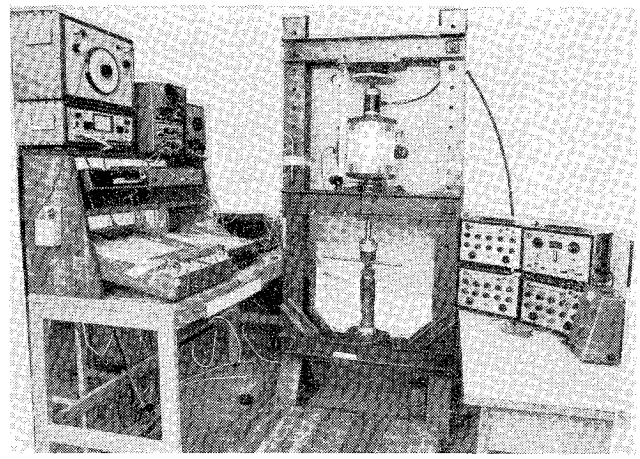

Fig. 3 Test setup.

The buckling loads and modes of all the AB shells are summarized in Table 2. The vibration tests on shell AB1, which was excited acoustically, did not yield enough conclusive and consistent experimental results for meaningful correlation. It buckled nonviolently at $P_{exp} = 4700$ kg with $n = 9$, $m = 1$, and a relatively small drop in load to $P_{post} = 4150$ kg. This behavior aroused the first suspicions of a possible load eccentricity which were, however, discarded, since all of the attention was devoted to improvement of the vibration technique.

The second test, on shell AB3, already used the narrow band filter and yielded fairly consistent results suitable for correlation attempts. Details are presented in the extended version of the paper.[21] Again, buckling was relatively gentle with the load dropping from $P_{exp} = 3400$ kg (with $n = 8$, $m = 1$) to $P_{post} = 2970$ kg.

Table 2 Theoretical and experimental buckling loads and modes

Shell	Experiment P_{exp}, kg	Experiment P_{post}, kg	*SS3* P_{cr}, kg	*SS4* P_{cr}, kg	*C4* P_{cr}, kg	P_{sp}, kg	ρ_{SS3}	ρ_{SS4}	ρ_{C4}	ρ_{sp}
AB1	4700	4150	4996	6554	9300	—	0.94	0.72	0.51	—
	9/1[a]		12/1	12/1	12/1					
AB2	4900	4040	4828	6358	8990	5260	1.01	0.77	0.55	0.93
	9/1		12/1	12/1	12/1	12/1				
AB3	3400	2970	3967	5942	7230	4980	0.86	0.58	0.47	0.68
	8/1		10/1	11/1	12/1	11/1				
AB4	3615	3038	3955	5929	7204	5260	0.91	0.61	0.50	0.69
	8/1		10/1	11/1	12/1	11/1				
AB5	3580	3000	3833	5574	7044	4130	0.93	0.64	0.51	0.87
	9/1		11/1	12/1	12/1	11/1				
AB6	4025	2250	3687	5425	6489	5340[b]	1.09	0.74	0.62	0.75[b]
	9/1		11/1	12/1	12/1	12/1				

[a] The numbers below the buckling loads represent the buckling mode n/m. [b] No noticeable load eccentricity observed.

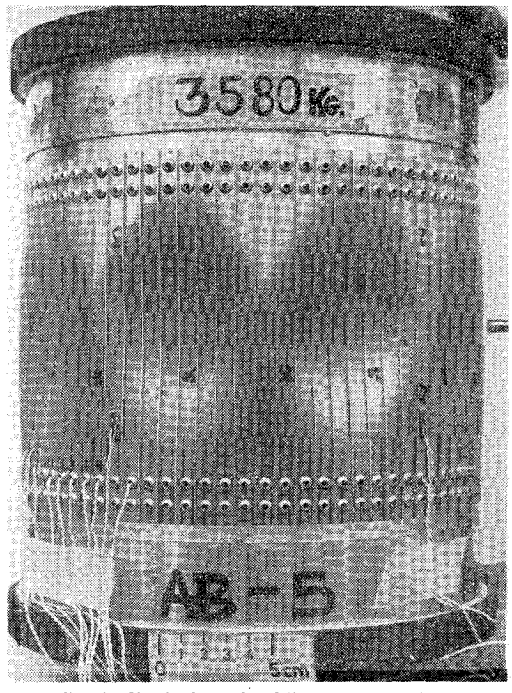

Fig. 4 Typical postbuckling pattern—AB5.

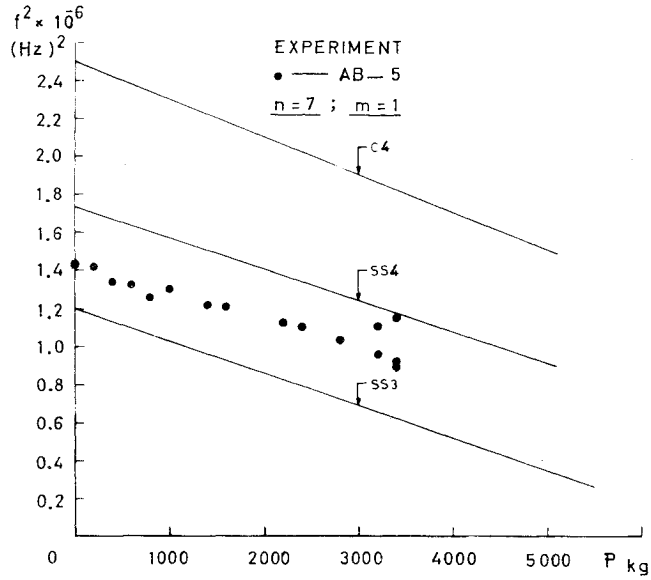

Fig. 5 Frequency squared vs axial load—shell AB5 for $n = 7$, $m = 1$.

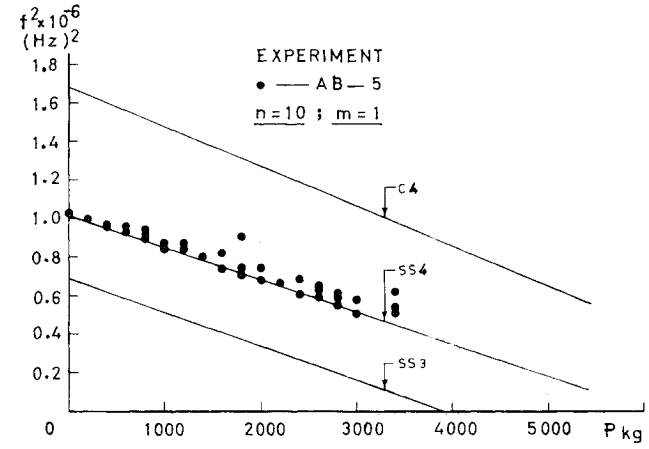

Fig. 6 Frequency squared vs axial load—shell AB5 for $n = 10$, $m = 1$.

On the third shell tested, AB4 (a twin of AB3), the direct-contact excitation technique—evaluated in the comparison tests just discussed—was already employed. It yielded consistent results which provided extensive data for the correlation studies (for details see Ref. 21). Buckling at $P_{exp} = 3615$ kg with $n = 8$, $m = 1$ was again nonviolent and $P_{post} = 3040$ kg.

By this time the suspicion of load eccentricity had grown. In the next shell, AB2 (a twin of AB1), verification of the load eccentricity was, therefore, attempted. Two pairs of five closely spaced strain gages were bonded as close as possible to the edges of the shell. Surprisingly, no significant bending strains, which would verify the suspected load eccentricity, were observed, though the buckling behavior again resembled a typical case of considerable load eccentricity. The buckling load was $P_{exp} = 4900$ kg with $n = 9$, $m = 1$ and $P_{post} = 4040$ kg. Close examination of the position of the special gages led to the conclusion that because of the nature of the joint, they were too far from the edge to show the very local edge bending strains typical of load eccentricity.[9]

In the last two shells of the series, AB5 and AB6, special recesses therefore were cut in the riveted end rings to permit measurement very close to the edge of the shell (among the rivets). The strips were bonded in pairs to allow separate measurement of bending and compressive strains. In shell AB5 significant bending strains were found which diminished rapidly away from the edge,[21] verifying the suspected external load eccentricity and explaining also the failure to observe similar bending strains in AB2.

The vibrations of shell AB5 yielded very consistent results (see Figs. 5 and 6). Note that for clarity the theoretical lines for different elastic axial and rotational restraints,[2,6-8] k_1 between *SS3* and *SS4*, and k_4 between *SS4* and *C4*, respectively, have been omitted from these figures. Furthermore, whereas usually the effective springs representing the boundary conditions were not affected by the choice of n,[2,6-8] here in the AB shells the corresponding effective springs seem to increase with n. This property is discussed in detail in the next section and found to be a means of identification for load eccentricity. If there were no load eccentricity effects, the vibration correlation technique[2,6-8] would now be applied to obtain improved predictions of the buckling loads. Straightforward application of the method would mean determination of k_1 from observed f^2 at the chosen n,m in an appropriate f^2 vs k_1 graph (see, for example, Fig. 4 in Ref. 7) and finding the corresponding P_{sp} in the accompanying P vs k_1 curve (for example like Fig. 5 in Ref. 7). In the presence of load eccentricity the method has to be modified as shown in Sec. IV.

Shell AB5 buckled gently at $P_{exp} = 3580$ kg with $n = 9$, $m = 1$ and $P_{post} = 3000$ kg (see Fig. 4).

In Figs. 5 and 6 there is some scatter in the measured frequencies. As the scatter appears to be larger with an increase in axial load, it may be suspected that nonlinear amplitude effects, which become more pronounced with an increase in axial load, are the cause of this scatter. However, since the amplitudes of the vibrations in the present tests were kept small, and similar scatter appeared in other tests also at small axial loads,[2,7,8] the scatter in the frequencies is probably due to other experimental effects.

In shell AB6, the closely spaced strain gages near the edge yielded bending strains similar in nature to those found in AB5 but of much smaller magnitude. Indeed the behavior of this shell differed noticeably from that of the other AB shells, indicating negligible load eccentricity. The height of the stringers in this shell d_1 was slightly smaller than the other shells of the series (see Table 1), which was one cause for the smaller load eccentricity here. The other causes are probably an accumulation of minor differences in tolerances and bolt tightness.

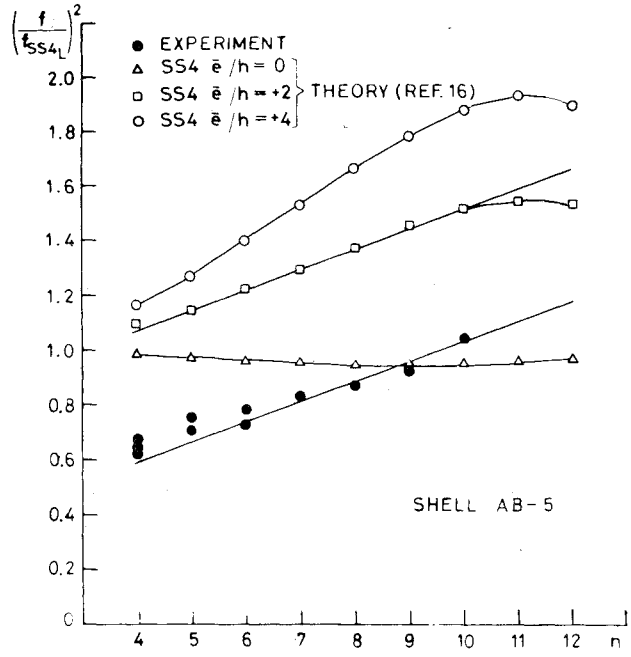

Fig. 7 Variation of frequency ratio squared with circumferential wavenumber n—shell AB5.

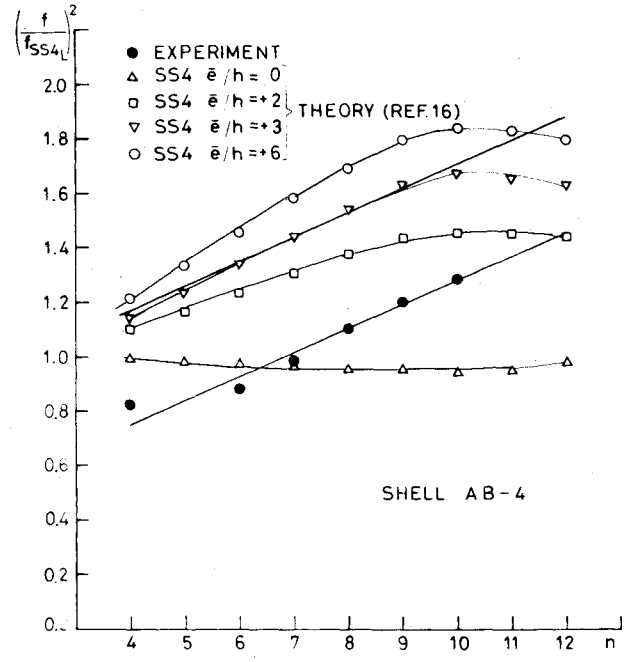

Fig. 8 Variation of frequency ratio squared with circumferential wavenumber n—shell AB4.

The vibrations of AB6 yielded consistent results,[21] which were very similar to those obtained in similar shells on laboratory-type boundary conditions without any load eccentricity.[2,6-8] The effect of n on k_l was considerably smaller than in the other AB shells.[21] Hence, it was assumed that the usual vibration correlation method could be applied to this shell. The shell buckled violently at $P_{exp} = 4025$ kg, with $n = 9$, $m = 1$, and a large drop in axial load was observed to $P_{post} = 2250$ kg.

IV. Eccentricity of Loading and Definition of Boundary Conditions

Eccentricity of loading, usually defined as the radial distance between the line of axial load application and the shell midskin, has been shown theoretically and experimentally to have considerable influence on the buckling load of stringer-stiffened cylindrical shells.[9,12,19,20,22-24] Since load eccentricity is usually not well defined a priori, as it often depends on the detailed behavior of the joint under load, its nondestructive determination, in practice, would significantly improve the prediction of buckling load.

The earlier work on shells with prescribed load eccentricity[9] has already shown that correlation between vibration and buckling is more complicated in this case, and that the effects of load eccentricity can obscure the otherwise fairly straightforward vibration correlation technique. Hence detection of load eccentricity from vibrations at low loads, in order to separate boundary conditions with and without significant load eccentricity, is an essential step to make the correlation method a practical tool.

Already in the earlier study on load eccentricity[9] a significant dependence of vibration behavior on the circumferential wave number was noted. However, only after some thorough study of the present test results did the apparently salient property, which distinguishes the vibrations under eccentric loading, emerge. This property is a noticeable relative increase in the measured frequency squared with the number of circumferential waves n of the vibration pattern. For AB5, for example, this can be seen by comparison of Figs. 5 and 6, noting the marked stiffening in the apparent effective elastic restraining for $n = 7$, $m = 1$ in Fig. 5 to $n = 10$, $m = 1$ in Fig. 7. This property becomes more pronounced if one plots the frequency ratio squared $(f/f_{SS4_L})^2$ vs n, as shown for shell AB5 in Fig. 7. The frequency ratio here is the ratio of the experimentally observed frequency to that predicted by linear theory[7,13] for *SS4* boundary conditions. If one now plots the corresponding theoretical freqency ratio squared for some likely values of load eccentricity where $f_{SS4+\bar{e}}$ is the frequency computed with BOSOR 3[16] (which considers nonlinear prebuckling deformations) for *SS4* boundary conditions in the presence of load eccentricity $\bar{e}$, the same property becomes evident. One can easily find a load eccentricity $(\bar{e}/h)$ that has the same slope as the experimental one. Note that the experimental frequency ratios are lower than the corresponding theoretical ones, since they also include imperfections which are not taken into account in the theoretical predictions, as well as the difference in the comparison. In Fig. 8, the frequency ratios squared for shell AB4 are plotted in a similar manner, again demonstrating the definite slope with n which identifies significant load eccentricity.

In order to verify this salient property which distinguishes the vibrations in the presence of load eccentricity, the results of earlier tests[9] of similar shells, RO shells on laboratory-type boundary conditions with prescribed load eccentricity, were plotted in the same manner. Figure 9 shows the frequency ratio squared vs n for shell RO-29, with prescribed external load eccentricity $(\bar{e}/h) = 4.35$, and the similarity with Figs. 7 and 8 is immediately evident. When the frequency ratio is plotted for the "twin" shell RO-28, with zero load eccentricity, in Fig. 10, the absence of the positive slope identifying external eccentricity is apparent. Note that the theoretical frequency ratio in Fig. 10 is slightly below 1.0, the difference representing the effect of nonlinear prebuckling deformations.

A partial physical explanation of this observed increase in frequency ratio squared with increase in n could be along the following lines: It has been shown[25] that for isotropic shells the relative portions of the strain energy due to bending and stretching strongly depend on n. For small n, stretching predominates and for large n, bending provides the prime component. One also may assume a similar division of predominance for stringer-stiffened shells. Now, eccentricity of loading increases the effective moment of inertia of the stringer shell combination and increases the resistance to axial bending. Hence, where bending energy predominates (for

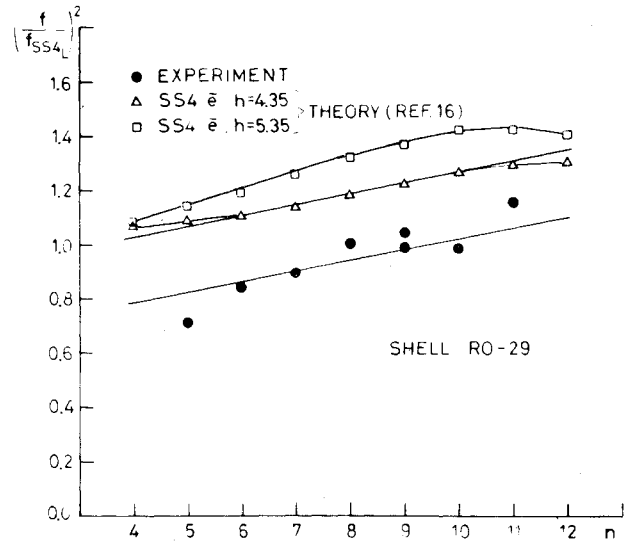

Fig. 9 Variation of frequency ratio squared with circumferential wavenumber n—shell with prescribed eccentricity RO-29.

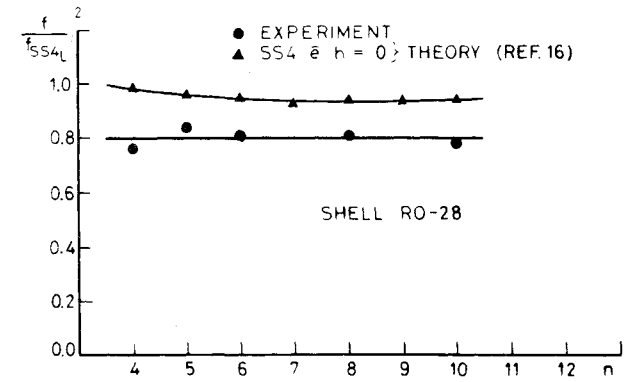

Fig. 10 Variation of frequency ratio squared with circumferential wavenumber n—shell with prescribed zero eccentricity RO-28.

large n), the presence of load eccentricity means higher stiffness and, therefore, increased frequency of vibration. For small n, where stretching energy predominates, load eccentricity will not raise the frequency in the same manner. Hence, the increase in frequency ratio with n that is observed in Figs. 7-9. This effect occurs primarily for *SS4* boundary conditions, since the eccentric load application points are axially restrained and vibration is, therefore, constrained to be about the eccentric axis with the resulting larger moment of inertia. In the case of *SS3* boundary conditions, there is no axial restraint, and the shell can still vibrate approximately about its centroidal axis without increased effective moment of inertia, though the load is applied eccentrically. For buckling, a "barreling" or, in the case of external load eccentricity, a negative barreling effect,[23] comes into play which may counteract the increase in effective moment of inertia. The physical explanation is, therefore, more complicated for the buckling phenomenon.

Since the verification of the vibration property which permits nondestructive identification of load eccentricity is important for making the method more reliable, two series of RO shells have been evaluated,[21] and additional tests of shells with prescribed load eccentricity have been carried out. All the data reduced from the RO shells[21] and the preliminary results of the additional tests verify the slope property, conclusively.

The vibration correlation technique provides, therefore, a nondestructive means for detecting an unknown load eccentricity in the presence of other boundary effects.

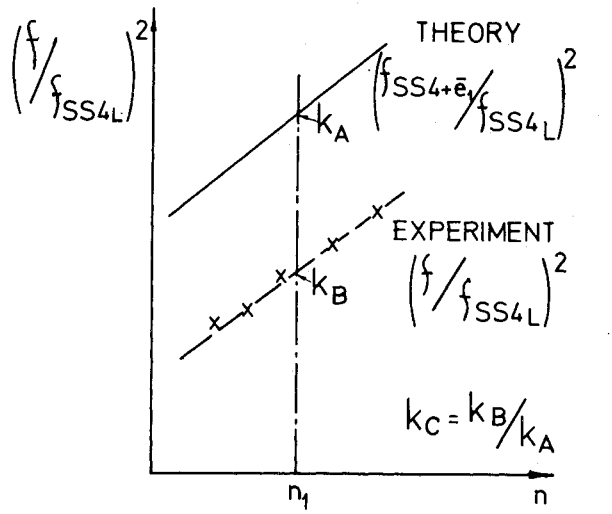

Fig. 11 Determination of equivalent boundary condition factor for eccentrically loaded shells.

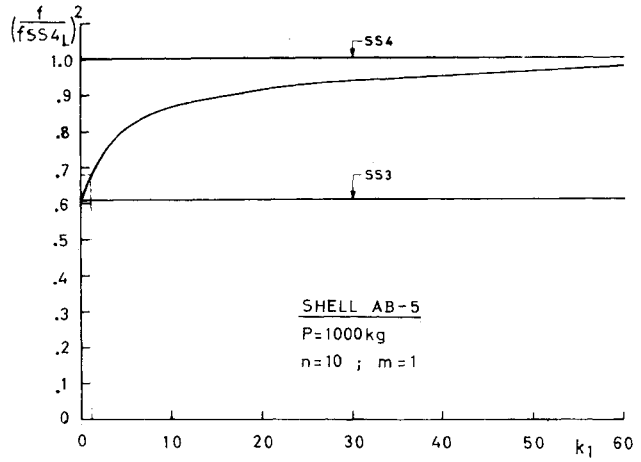

Fig. 12 Influence of elastic axial restraint k_1 on the vibrations of shell AB5, $n = 10$, $m = 1$.

In order to define now the boundary conditions in the presence of load eccentricity, the vibration correlation method has to be modified. The frequency ratios shown in Figs. 7-10 are all referred to *SS4* boundary conditions, since the modified method tacitly assumes that the real boundary conditions in the presence of significant load eccentricity are not far from *SS4* and, hence, *SS4* can be used for reference. When the actual boundary conditions are far from *SS4*, the method is still effective, but has a more empirical flavor.

The details of the method are shown schematically in Fig. 11. To a typical plot of experimental frequency ratios squared vs n (like Figs. 7-9), a theoretical curve (calculated with BOSOR 3 or 4) is "fitted" for a load eccentricity $(\bar{e}/h)_1$ that has the same slope. An appropriate value of n is chosen, say n_1, which is usually taken as that at which buckling is predicted, or a value slightly below it (based on the observation that the experimental n in most tests on stiffened shells is just slightly below the theoretically predicted one[7,8,18]). For n_1, the effective theoretical frequency ratio squared, k_A, and the corresponding experimental one, k_B, are read off the curves. Since the experimental values include the boundary effects and also part of the influence of imperfections, the ratio $k_C = (k_B/k_A)$ represents an equivalent boundary condition factor. With this k_C, the procedure then follows the correlation method in its regular form. An equivalent frequency squared $f^2 = k_C \cdot (f_{SS4L})^2$ replaces the measured frequency squared. Consider, for example, AB5:

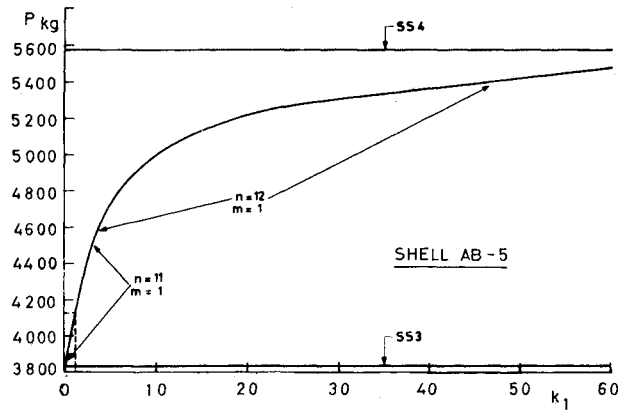

Fig. 13 Influence of elastic axial restraint k_1 on the buckling load of shell AB5.

Figure 12 shows the equivalent frequency ratio squared $(f/f_{SS4I})^2$ vs k_1, the equivalent axial elastic restraint for this shell. Note that k_C is equivalent to $(f/f_{SS4L})^2$ in the case when there is no load eccentricity. From Fig. 7 one obtains for $n=10$, $k_A=1.55$, and $k_B=1.05$, hence, $k_C=k_B/k_A=0.68$. The corresponding k_1 in Fig. 12 is 1.2.

From Fig. 13, the usual P_{sp} vs k_1 plot, this equivalent axial spring k_1 then yields $P_{sp}=4130$ kg and $\rho_{sp}=0.87$. The procedure was applied to shells AB2-AB5 and the results are given in Table 3 of Ref. 21, where the influence of the choice of n on the resultant ρ_{sp} is also studied. One observed that the influence is not large, and that choice of a larger n results in a conservative estimate for the "linearity."

The method outlined yielded consistent results for the AB shells (except AB1 which, as previously discussed, did not yield enough vibration data, and AB6 whose load eccentricity was neglected in its final evaluation). Having been extended to realistic boundary conditions that include unknown load eccentricities, the vibration correlation technique for definition of boundary conditions has become a practical tool for improved buckling load predictions.

One may note that there are significant differences in ρ_{sp} obtained for shells AB2-AB5 in Table 2. These differences are probably due to initial imperfections which, though less important for stiffened shells, still affect them. Work is in progress to correlate the measured initial imperfections with the variations in buckling load.

The method could, however, be improved if calculations of vibrations and buckling in the presence of load eccentricity were possible for shells on elastically restrained boundaries. Computation routines extending BOSOR 4 to this case are being developed.

V. Conclusions

The following conclusions can be drawn from the results discussed:

1) The vibration correlation technique for definition of the boundary conditions has been extended to stiffened shells on realistic boundary conditions. Six stringer-stiffened shells on end rings simulating typical missile joints have been tested and evaluated. The main problem encountered was the "lumping" of different boundary effects and, in particular, the presence of unknown load eccentricities.

2) In the data reduction of the tests, a salient property which distinghishes the vibrations in the presence of load eccentricity has been observed. This property is a large increase in the frequency ratio squared $(f/f_{SS4L})^2$ with the number of circumferential waves n of the vibration pattern, which does not occur in the absence of load eccentricity.

3) After verification with theory and with tests of shells having prescribed load eccentricity, a nondestructive method for detection of unknown load eccentricities in the presence of other boundary effects is obtained.

4) The vibration correlation technique for definition of boundary conditions has been modified to account for the presence of load eccentricity, once it has been detected. With this extension, the method has become a practical tool for improved buckling load predictions.

5) Further studies are in progress to reconfirm the load eccentricity effects on vibrations and to extend the computation routines to cases of load eccentricity and elastic restraints.

VI. Acknowledgments

The authors wish to thank A. Grunwald, A. Klausner and S. Nachmani of the staff of the Aeronautical Structures Laboratory for their dedicated assistance with the experimental work. They also wish to thank A. Rosen for useful discussions, J. Gil for his assistance with computations, R. Rabinovich for the preparation of the figures, and E. Youdim and R. Zmirin for the typing of the manuscript.

References

[1] Singer, J., "Buckling of Integrally Stiffened Cylindrical Shells—A Review of Experiment and Theory,," *Contributions to the Theory of Aircraft Structures*, Delft University Press, Delft, The Netherlands, 1972, pp. 325-357.

[2] Singer, J. and Rosen, A., "Influence of Boundary Conditions on the Buckling of Stiffened Cylindrical Shells," *Buckling of Structures, Proceedings of IUTAM Symposium*, Harvard University, Cambridge, Mass., June 1974; Springer-Verlag, Berlin, pp. 227-250, 1976.

[3] Penzes, L. E., "Effect of Boundary Conditions on Flexural Vibrations of Thin Orthogonally Stiffened Cylindrical Shells," *Journal of Acoustical Society of America*, Vol. 42, April 1967, pp. 901-903.

[4] Sewall, J. L. and Naumann, E. C., "An Experimental and Analytical Vibration Study of Thin Cylindrical Shells with an without Longitudinal Stiffeners," NASA TN D-4705, Sept. 1968.

[5] Rosen, A. and Singer, J., "Vibrations of Axially Loaded Cylindrical Shells," *Journal of Sound and Vibration*, Vol. 34, No. 3, June 1974, pp. 357-378.

[6] Singer, J. and Rosen, A., "Design Criteria for Buckling and Vibration of Imperfect Stiffened Shells," *ICAS Proceedings 1974, Proceedings of the 9th Cong. of the International Council of the Aeronautical Sciences*, Haifa, Israel, Aug. 1974; Weizmann Science Press of Israel, Jerusalem, pp. 495-517, 1974.

[7] Rosen, A. and Singer, J., "Vibration of Axially Loaded Stiffened Cylindrical Shells with Elastic Restraints," *International Journal of Solids and Structures*, Vol. 12, Aug. 1976, pp. 577-588.

[8] Rosen, A. and Singer, J., "Further Experimental Studies of Vibrations of Axially Loaded Stiffened Cylindrical Shells," TAE Rept. 210, Technion, Israel Inst. of Technology, Dept. of Aeronautical Engineering, May 1975.

[9] Rosen, A. and Singer, J., "Vibrations and Buckling of Eccentrically Loaded Stiffened Cylindrical Shells," *Experimental Mechanics*, Vol. 16, March 1976, pp. 88-94.

[10] Abramovich, H., Singer, J., and Grunwald, A., "Correlation between Vibrations and Buckling of Stiffened Cylindrical Shells under External Pressure and Combined Loading," TAE Rept. 326, Technion, Israel Inst. of Technology, Dept. of Aeronautical Engineering, Dec. 1977.

[11] Singer, J., "Buckling, Vibrations and Postbuckling of Stiffened Metal Cylindrical Shells," *Proceedings of BOSS 76*, 1st International Conference on Behavior of Off-Shore Structures, Norwegian Institute of Technology, Trondheim, Norway, Aug. 1976, pp. 765-786.

[12] Weller, T., Singer, J., and Batterman, S. C., "Influence of Eccentricity of Loading on Buckling of Stringer-Stiffened Cylindrical Shells," *Thin-Shell Structure, Theory, Experiment and Design*, Y. C. Fung and E. E. Sechler, (Eds.), Prentice-Hall, Englewood Cliffs, N.J., 1974, pp. 305-324.

[13] Rosen, A. and Singer, J., "Vibrations of Axially Loaded Stiffened Cylindrical Shells: Part I—Theoretical Analysis," TAE Rept. 162, Technion, Israel Inst. of Technology, Dept. of Aeronautical Engineering, Feb. 1974.

[14] Baruch, M. and Singer, J., "Effect of Eccentricity of Stiffeners on the General Instability of Stiffened Cylindrical Shells under Hydrostatic Pressure," *Journal of Mechanical Engineering Science*, Vol. 5, No. 1, March 1963, pp. 23-27.

[15] Singer, J., Baruch, M., and Harari, O., "On the Stability of Eccentrically Stiffened Cylindrical Shells under Axial Compression," *International Journal of Solids and Structures*, Vol. 3, No. 4, July 1967, pp. 445-470.

[16] Bushnell, D., "Stress, Stability and Vibration of Complex Shells of Revolution," *Analysis and Users' Manual for BOSOR 3*, Lockheed Missiles & Space Co., Rept. N-5J-69-1, Sept. 1969.

[17] Bushnell, D., "Stress, Stability and Vibration of Complex Branched Shells of Revolution," *Analysis and Users' Manual for BOSOR 4*, Lockheed Missiles & Space Co., Rept. LMSC D-243605, March 1972.

[18] Weller, T. and Singer, J., "Experimental Studies on Buckling of 7075-T6 Aluminum Alloy Integrally Stringer-Stiffened Shells," TAE Rept. 135, Technion R&D Foundation, Haifa, Israel, Oct. 1971.

[19] Stuhlman, C. E., De Luzio, A., and Almroth, B., "Influence of Stiffener Eccentricity and End Moment on Stability of Cylinders in Compression," *AIAA Journal*, Vol. 4, May 1966, pp. 872-877.

[20] Block, D. L., "Influence of Discrete Ring Stiffeners and Prebuckling Deformations on the Buckling of Eccentrically Stiffened Orthotropic Cylinders," NASA TN D-4283, Jan. 1968.

[21] Singer, J. and Abramovich, H., "The Influence of Practical Boundary Conditions on the Vibrations and Buckling of Stiffened Cylindrical Shells," TAE Rept. 288, Technion, Israel Inst. of Technology, Dept. of Aeronautical Engineering, Feb. 1978.

[22] Almroth, B. O. and Bushnell, D., "Computer Analysis of Various Shells of Revolution," *AIAA Journal*, Vol. 6, Oct. 1968, pp. 1848-1855.

[23] Hutchinson, J. W. and Frauenthal, J. C., "Elastic Post-Buckling Behavior of Stiffened and Barreled Cylinders," *Journal of Applied Mechanics*, Vol. 36, Series E, No. 4, Dec. 1969, pp. 784-790.

[24] Chang, L. K. and Card, M. F., "Thermal Buckling Analysis for Stiffened Orthotropic Shells," NASA TN D-6332, April 1971.

[25] Arnold, R. N. Warburton, G. B., "Flexural Vibrations of the Walls of Thin Cylindrical Shells Having Freely Supported Ends," *Proceedings of Royal Society of London*, Vol. 197, Ser. A, 1949, pp. 238-256.